JOURNAL OF OPTOELECTRONICS AND ADVANCED MATERIALS Vol. 10, No. 8, August 2008, p. 2129 - 2133

Effect of crystallization on the optical properties of $Se_{0.8}S_{0.2}$ amorphous films

M. ABDEL RAFEA*, HUDA FARID
Institute of Advanced Technology & New Materials, Mubarak City for Scientific Research & Technology Applications
P.O. Box 21934 Universities and Research Centers District, New Borg El Arab City, Alexandria, Egypt

$Se_{0.8}S_{0.2}$ glassy films of thickness 583 nm have been prepared by thermal vacuum evaporation technique. Annealing of the films shows that the crystallization process starts at T= 333 K and nanostructured film is formed. The increase of the annealing temperature to 373 K increases the crystallite size to 24 nm. Orthorhombic crystalline system was identified for the annealed films. SEM micrographs show that films consist of two parallel surfaces and the thickness was determined by cross section imaging. The optical transmittance is characterized by interference patterns as a result of these two parallel surfaces, besides their average value at longer wavelength decreases as a result of annealing process. The band gap, E_g is red shifted due to crystallization by annealing. The change of E_g from the amorphous value to the crystalline one is not sharp. A relatively slow decrease in E_g intermediate annealing temperature was observed. This change was explained in the energy gap confinement behavior of the nanostructured films and the phenomena was discussed in the Brus`s model. The optical refractive index increases suddenly when the system starts to be crystallized by annealing.

(Received March 22, 2008; accepted June 30, 2008)

Keywords: Chalcogenide glasses, Thermal vacuum evaporation, Annealing, Crystallization, Nanostructured films, Optical properties

1. Introduction

Chalcogenide glasses have received a great deal of attention for the last two decades due to their technological applications, namely electronic, optoelectronic, optical and memory switching devices such as optical recording media. Short laser pulse crystallizes the amorphous layer, which change the optical parameters of the chalcogenide film, while longer laser pulse melt the area of illumination and then solidified as amorphous phase. The optical absorption edges of the amorphous and crystalline are considered the two bit binary storage data and could be detected optically. Another applications, amorphous Se has been found to have tremendous potential in xerography applications. The glassy state Se-S exhibits an electronic conductivity of p-type semiconductor. The addition of S to Se leads to a decrease in the density as well as an increase in the glass transition temperature [1-2]. Partial replacement of the chalcogenide system by arsenic in the $As_{33}S_{67-x}Se_x$ glass system of x = 0 - 67, the increase of Se content decreases the band gap from 2.45 to 1.8 eV. Also a red shift in the absorption edge takes place by annealing the films at T=423 K for 30 and 60 min [3]. P-type Se_{100-x} S_x films were deposited on n-Si with x= 0.25- 7.28, a good rectifying characteristics were obtained. The photovoltaic parameters of this type of solar cells were determined with efficiency 4.28 % which decreases as x increases [4]. In the $As_{40}S_{60-x}Se_x$ glass system, the glass transition temperature decreases from 488 to 387 K as x increases from 0 to 60, besides large red shift is obtained in absorption curves [5,6]. The annealing temperature dependence of the band gap in $Se_{0.85}Te_{0.15}$ glass films shows a slight increase in E_g from 1.09 to 1.16 eV as annealing temperature increases up to 353 K. This behavior was explained on the basis of the Mott - Davis model for the density of states in amorphous solids. When annealing temperature increases from 353 to 385K, E_g decreases gradually to a value of 0.67 eV [7]. This phenomena was observed also in other glassy systems SbSe [8] and GeSeTe [9] with different values of band gap and temperature ranges. This gradual decrease in E_g was explained to be a result of an amorphous–crystalline phase transformation. The decrease of E_g by annealing is an interesting behavior specially for optical recording memory system, although it is important in this application to shift the absorption edge sharply, the above shift of E_g due to crystallization for example in Ref.[7] is not sudden change from 1.16 to 0.67 eV, While the system structure changes from amorphous to crystalline states. In this work, we study the optical properties of $Se_{0\cdot8}S_{0.2}$ films as a function of annealing temperature in the range close to the crystallization temperature and study intensively the change of E_g with annealing temperature.

2. Experimental

Selenium and sulfur elements of purities “5N Acros-Organics”, were used to prepare $Se_{0.8}S_{0.2}$ system. Fine powder of Se an S were mixed and mechanically alloyed in a hardened agate in order to obtain homogeneously well mixed powder "this method was used in Ref. [10]". Pellets of diameters 10 mm and thickness 2 mm were prepared by hydraulic press at 8 kN/cm^2 under vacuum. 200 mg of the pressed material was evaporated in a Mo boat under vacuum of 8×10^{-6} Torr using a standard BOC-Edwards A306 Auto coating unit with conventional rotary and turbo molecular pumps.

Glass substrate was cleaned several times using ultrasonic cleaner, detergent, Double distilled water and

final washing with ethyl alcohol. Before evaporation, a glow discharge process took place for further substrate surface cleaning in the vacuum system. A rotating substrate holder was used with adjusted and fixed rotating speed that produces films with high homogeneity. The thickness of the films was determined by thickness monitor during the deposition. The evaporation rate was in the range 3-4 Å/sec. The substrate temperature was at 300 K during evaporation and evaporation rate. The films were annealed in the temperature range 300-373 K for one hour in vacuum oven.

The structure of the deposited films was studied using Shimadzu XRD 7000 maxima powder diffraction at the conditions "tube voltage 30 KV, current 30 mA and wavelength CuKα_1, λ=1.5406 Å using Ni filter. The scan range 2θ=10-80^o and scan speed 2^o/min. SEM of type Jeol-JSM-636 OLA was used to study the surface morphology of the deposited films. The cross sectional image of the film and the substrate also determine the film's thickness at different points of a broken edge the average film thickness was found to be 583 nm. The optical transmittance of the films was measured using SPECTRO UV–VIS DOUBLE BEAM UVD2950 PC SCANNING LABOMED spectrophotometer of spectral range 190-1100 nm and a reference substrate was used.

3. Results and discussions

3.1 XRD measurements

The as deposited films and those annealed at 318 K were observed to be amorphous. Fig.(1.a) shows a representative XRD chart of film annealed at 318 K. There is no diffracted peak in the chart, which indicates that the structure of the films is amorphous, this result was also obtained in a previous study for $Se_{1-x}S_x$ in the composition range 0.0-0.4 that all deposited films are amorphous. Crystallization process is obtained by annealing of the films above 318 K [11]. Fig.(1.b) represents the XRD measurements at different temperature up to 373 K, each curve in the figure was normalized and plotted in the same group of curves with maximum intensity scale 100 % in order to compare with the other curves. There are five characteristic peaks are obtained from the charts, a special software ICCDview [12] are used to identify the peaks with the corresponding standard. Orthorhombic crystallographic system is obtained with many absent peaks due to films preferred orientations during the growth process. The nearest system available in the ICCDview data bank is $Se_{72.86}S_{27.14}$ with a card ID [01-078-0266]. Also small shift on the inter-atomic spacing were found due to a small difference between the film composition and the standard card. The crystallization process starts with considerable high intensities of the peaks (310) and (221). As The annealing temperature increases, these peaks intensities decreases in compared with the other peaks. The opposite behavior was observed in the peaks (320), (420) and (260) with a highest intensity at (420). These two behaviors can be understood in the bases of the nucleation and formation of crystallites the directions of the last peaks. The average crystallite size was calculated using the well known Scherrer`s equation:

$$D = \frac{0.94\lambda}{\sqrt{\beta^2_{sample} - \beta^2_{silicon}}.\cos\theta} \quad (1)$$

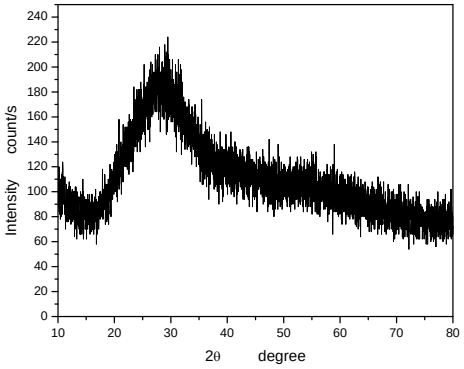

a

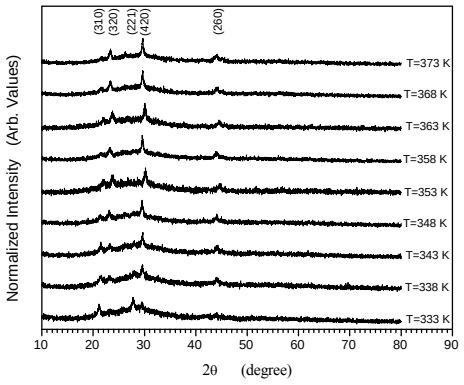

b

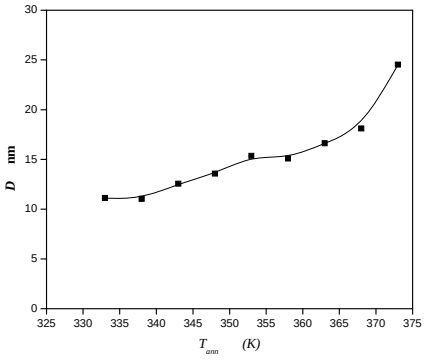

c

Fig. 1. a XRD measurement of $Se_{0.8}S_{0.2}$ film annealed at 318 K as representative chart for amorphous films. b. XRD measurements of $Se_{0.8}S_{0.2}$ films annealed at temperatures from 333 to 373 K. c. crystallite size dependence upon the annealing temperature for $Se_{0.8}S_{0.2}$ films.

Where D is the crystal size, λ is the x-ray wavelength, β_{sample} and $\beta_{silicon}$ are the width at half maxima of the broadened peaks of the sample and a silicon crystal respectively. The use of silicon free defect crystal measures the instrumental broadening. The low scanning

rate of the 2θ and neglecting the micro strain of the non thermal stressed films (our case) enable to calculate the crystallite size using Eqn.(1). Fig.(1.c) shows the crystallite size dependence upon the annealing temperature. Small increase in crystallite size was obtained in the annealing temperature range 338-363 K due to nucleation and crystallite formation, in this range the size of crystallites are in the range 11-16 nm. At annealing temperature 373 K, the crystallite size increases to 24 nm due to growth. In this temperature range 318-373 K a nanostructured films are obtained.

3.2 Scanning electron microscope

Scanning electron micrograph of the as deposited films shows that the film possesses good surface properties, there is no characteristic morphologies, cracks or grains appear, this may be logic for amorphous films especially the deposition technique produces high quality films although we investigate The surface at high magnification (100,000) as shown in Fig.(2.a). The most important measurement is the cross sectional image for the thickness measurement as shown in Fig.(2.b). The substrate was cleaved to obtain an edge. The electron beam scans the substrate-film interface which can resolve the two different materials (i.e. the glass substrate and the film). Using the SEM facility for distance measurements program at the film boundaries, the average thickness is then calculated which was found to be 583±20 nm. Besides, a good film adhesion with the substrate is observed.

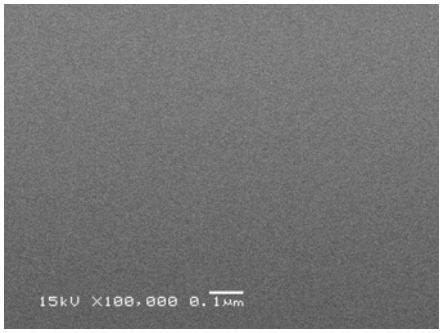

a

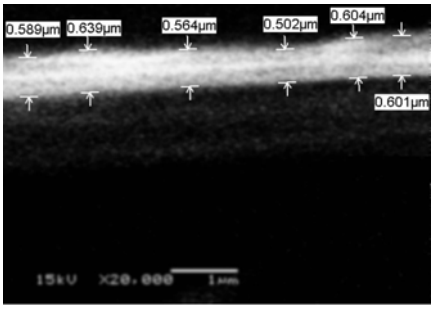

b

Fig. 2. a SEM of the as deposited $Se_{0.8}S_{0.2}$ film. b. Cross sectional SEM of the as deposited $Se_{0.8}S_{0.2}$ film.

3.3 Optical measurements

The optical transmittance was measured for films at different annealing temperatures. Fig.(3.a) shows the optical transmittances of four selected graphs as representative curves. It is observed that as the annealing temperature increases, the average optical transmittance decreases. The optical absorption edge is also shifted towards the longer wavelength (red shift) which indicates that the energy gap of the films decreases by annealing. The optical constants were determined for the annealed films using the envelope method which explained elsewhere [13]. The band gap was calculated from the optical transmittance (T), absorption coefficient (α) and thickness (d) relationship:-

$$T = \frac{I}{I_o} = e^{-\alpha d} \tag{2}$$

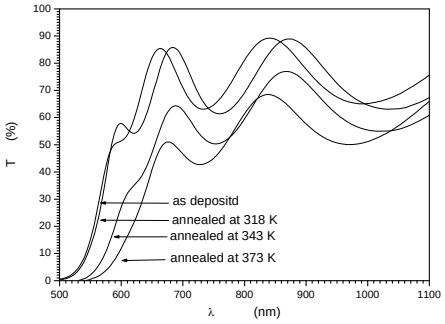

a

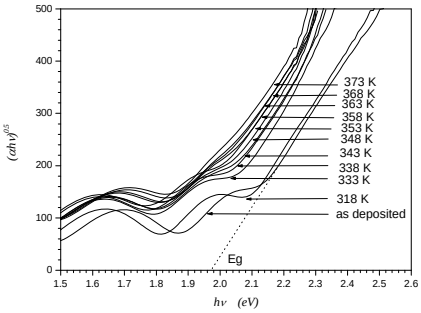

b

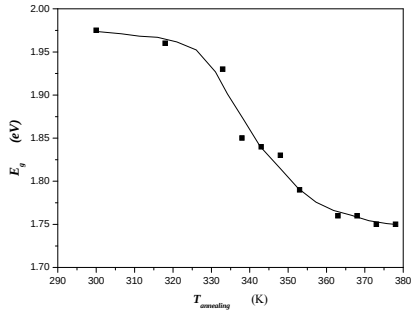

c

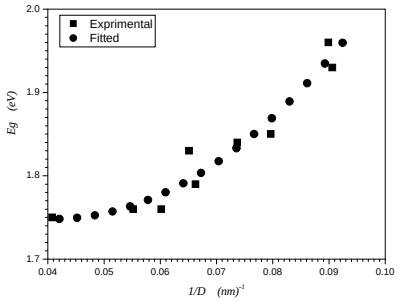

d

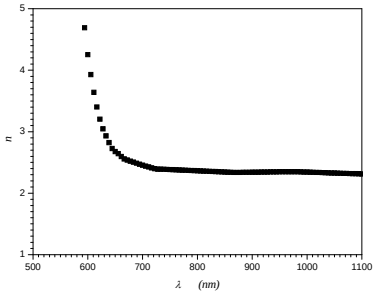

e

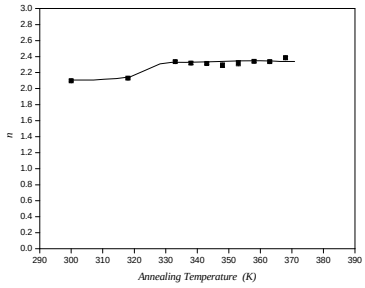

f

Fig. 3. a. Optical transmittance of four representative curves annealed at different temperature, b. $(\alpha h\nu)^{0.5}$ vs $h\nu$ for indirect transition for E_g determination, c. Dependence of E_g upon the annealing temperature, d. Dependence of E_g upon the crystallite size of $Se_{0.8}S_{0.2}$ film, e. Refractive index of representative sample annealed at 368 K, f. Refractive index dependence upon the annealing temperature.

Eqn.(2) has an approximation due to reflection, its effect is negligible because all samples are the same in thickness and substrate type so that they possess the same reflection factor. The absorption coefficient dependence upon the incident photon energy is then given by:-

$$\alpha = B\frac{\left(h\nu - E_g\right)^2}{h\nu} \qquad (3)$$

chalcogenide system is characterized by indirect transition so that the exponent of the $h\upsilon - E_g$ is square and B is a constant. The plot of $(\alpha h\nu)^{0.5}$ vs $h\nu$ results the absorption edges as shown in Fig.(3.b). The intercept of the edge with the photon energy axis is the optical band gap. The calculated band gaps was plotted against the annealing temperature in Fig.(3.c). The annealing temperature dependence upon the band gap is characterized by characteristic three regions. At low annealing temperature, the band gap decreases slowly. A gradual decrease in the band gap was observed in the intermediate temperature range then saturation was reached at higher temperature. The red shift of the band gap can be discussed in the crystallization mechanism. The glassy phase and crystalline one possess energy gaps that appear at the lower and higher annealing temperature as explained by XRD measurements. This behavior agrees well with Soltan et al [7] for the crystallization process of Se-Te glassy system, while the gradual decreasing of energy gap in the intermediate region of annealing temperature was not discussed before. In nano structured materials, if the crystallite size is too small to be compared with the Bohr exciton radius, a confinement effect of the band gap appears and a considerable increase in the energy gap is observed as suggested by Brus [14,15] which used in many nanostructured ZnSe and CdSe [16-19].

$$E_g(D) = E_{g.Bulk} + \frac{h^2}{8m_oD^2}\mu - \frac{1.8e^2}{4\pi\varepsilon_o\varepsilon_r D} - \frac{0.248\times 4\pi^2 e^4 m_o}{2h^2(4\pi\varepsilon_o\varepsilon_r)\mu} \qquad (4)$$

Where μ is the reduced effective mass $\{\mu=(1/m_e+1/m_h)^{-1}\}$ of the electron-hole respectively. has the physical meaning of each term in Eqn.(4). $E_g(D)$ is the band gap as a function of the crystallite size of the nanostructured material. $E_{g.bulk}$ is the band gap of the material in the microstructured form. The term $(h^2\mu/8m_oD^2)$ is the quantum localization (i.e. the kinetic energy term). It obviously shifts Eg(D) to higher energies proportionally to D^{-2}. The term $(-1.8e^2/4\pi\varepsilon_o\varepsilon_r D)$ is due to the screened Coulomb interaction between the electron and the hole, it shifts Eg(D) to lower energies proportionally to D^{-1}. The last term is size-independent term due to spatial correlation effects and is usually small in both the absolute value and the effect on Eg(D). Eqn.(4) is a second order equation on the crystallite size. Plotting the calculated band gap against the inverse of the crystallite size and fitting the resultant curve to the second order polynomial using Origin lab 6.1 software, the fitted curve is shown in Fig.(3.d). The second order polynomial fits well our results, the constants of each part of the equations can be easily determined by equating the terms of Eqn.(4) and the parameters of the fitting. The coefficient of first order of the inverse of the crystallite size is -6.52 and the coefficient of the second order one is 79.72. The sign of the coefficients of $1/D^2$ and $1/D$ in the fit function and Eqn.(4) are the same. This means that the gradual decrease of E_g in the intermediate region of the annealing temperature is governed only by the energy gap confinement effect of the nanostructured film. Furthermore, one of the important parameters is the reduced effective mass which can be determined by this method, it was found to be 0.587. In the system $Se_{0.85}Te_{0.15}$

in Ref. [7], and in other systems, crystallization of chalcogenide glasses was observed, the behavior was discuss only in the amorphous to crystalline transition while the intermediate region of the non sharp transition of E_g was an observation only. The importance of this analysis is to reach a full crystallization of the materials for example in some applications such as optical recording media. If the annealing by laser pulse is not sufficient to change the amorphous to micro crystalline state, the detection of this state optically will be difficult to resolve either the recorded bit is zero or one state so that the incident power of laser recorder on the media should be increased and optimized to make the material out of the confinement state.

The refractive index was calculated from the transmittance by the method Ref.[13]. One representative curve at annealing temperature 368 K was selected; all the other curves at different annealing temperatures have the same behavior. It is observed that near the fundamental absorption region, the refractive index increases sharply while at longer wavelength it nearly unchanged. The effect of annealing temperature on the refractive index is also studied at wavelength longer than the absorption edge as shown in Fig.(3.f). At low annealing temperature (T=300-318 K), the refractive index is close to 2.1 and jump to 2.32 at temperature higher than 318 K. This behavior is connected clearly with amorphous-crystallization transition as discussed in XRD measurements. The redistribution of Se-S atoms in crystallization process is mainly responsible for this sudden increase in refractive index.

4. Conclusions

In this work, the crystallization of $Se_{0.8}S_{0.2}$ chalcogenide glass film has some important conclusions. Deposition of the $Se_{0.8}S_{0.2}$ system at substrate temperature 300 K produces films with amorphous structure which was confirmed by XRD measurements. The films crystallize at annealing temperature above 333 K to Orthorhombic system, passing through nanostructure $Se_{0.8}S_{0.2}$ films. A high surface quality film was revealed by SEM and the thickness was determined by cross section image. The band gap of the films is changed by annealing due to crystallization with gradual decrease in the intermediate region of the annealing temperature. This change was discussed in the energy gap confinement behavior of nanostructured films. The phenomena was explained by the Brus`s model. The optical refractive index has a sudden change when the system starts to crystallize by annealing.

Acknowledgement

This work was carried out through the support from the Mubarak City for Scientific Research and Technology Applications (MUCSAT), projects program of the Institute of Advanced Technologies and New materials.

References

[1] Nadeem Musahwar, M. A. Majeed Khan, M. Husain, M. Zulfequar Physica B **396**, 81 (2007).
[2] A. M. A. EL-Barry Physica B **396**, 49 (2007).
[3] T. Kohoutek, T. Wagner, Mir. Vlcek, Mil. Vlcek, M. Frumar, Journal of Non-Crystalline Solids **352**, 1563 (2006).
[4] M. M. El-Nahass, H. E. A. El-Sayed, A. M. A. El-Barry, Solid-State Electronics **50,** 355 (2006).
[5] T. Cardinal, K. A. Richardson, H. Shim, A. Schulte, R. Beatty,K. Le Foulgoc, C. Meneghini, J. F. Viens, A. Villeneuve, J. Non-Crystalline Solids **256&257**, 353 (1999).
[6] K. Petkov, P.J.S. Ewen, J. Non-Crystalline Solids **249**, 150 (1999).
[7] A.S. Soltan, M. Abu EL-Oyoun, A.A. Abu-Sehly, A.Y. Abdel-Latief, Materials Chemistry and Physics **82**, 101 (2003).
[8] A. El-Korashy, A. Bakry, M.A. Abdel-Rahim, M. Abd El-Sattar, Physica **B 391**, 266 (2007).
[9] E.R. Shaaban, M. Abdel-Rahman, El Sayed Yousef , M.T. Dessouky, Thin Solid Films **515**, 3810 (2007).
[10] S.M. El-Sayed, Vacuum **65**, 177 (2002).
[11] M. Abdel Rafea, A. A. M. Farag, Chalcogenide Letters **5**(3), 27 (2008).
[12] International Centre for Diffraction Data software, ICDD View 2006 Release, Card ID: 01-078-0266, Match program SIIVE.
[13] E. R. Shaaban, N. El-Kabnay, A.M. Abou-sehly, N. Afify, Physica B **381**, 24 (2006).
[14] L. E. Brus, J. Chem. Phys. **79**, 5566 (1983).
[15] L. E. Brus, J. Chem. Phys. **80**, 4403 (1984).
[16] Biljana Pejova, Ivan Grozdanov, Materials Chemistry and Physics **90**, 35 (2005).
[17] Haiyan Hao, Xi Yao, Minqiang Wang, Optical Materials **29**, 573 (2007).
[18] Biljana Pejova, Ivan Grozdanov, Materials Letters **58**, 666 (2004).
[19] M. Abdel Rafea, J Material Science: Materials in Electronics **18**, 415 (2007).

*Corresponding author: m.abdelrafea@mucsat.sci.eg